science with current and future solar physics missions
ASI, february 1-3 2023

the reconstruction of electron maps by means of visibilities recorded by the Spectrometer/Telescope for Imaging X-rays on-board Solar Orbiter

michele piana
MIDA, dipartimento di matematica, università di genova
INAF – osservatorio astrofisico di torino

credits

- anna maria massone (UNIGE, co-PI STIX, all topics)
- paolo massa (UNIGE and western kentucky university, calibration, ground software)
- anna volpara (UNIGE, calibration, ground software)
- emma perracchione (POLITO, ground software)
- federico benvenuto (UNIGE, calibration, ground software)
- sara garbarino (UNIGE, ground software)

STIX: state of the art

image formation
(talk di anna volpara
domani)

Sub–coll. label	Sub–coll. number	Center X [mm]	Center Y [mm]	Slit width [mm]	Pitch front [mm]	Orientation front [deg]	Pitch rear [mm]	Orientation rear [deg]	m factor
10a	3	-62.5	-13.5	0.479	0.909644	151.481	0.999045	148.374	-1
10b	20	12.5	-27.5	0.479	0.951208	86.902	0.951208	93.098	1
10c	22	12.5	-73.5	0.479	0.909644	28.519	0.999045	31.626	1
9a	16	-12.5	-73.5	0.336	0.641967	170.363	0.691656	169.609	-1
9b	14	-12.5	-27.5	0.336	0.674193	107.937	0.656988	112.010	1
9c	32	62.5	-36.5	0.336	0.682197	51.702	0.649830	48.379	-1
8a	21	12.5	-50.5	0.236	0.453678	9.744	0.477944	10.270	1
8b	26	37.5	-13.5	0.236	0.457628	131.141	0.473450	128.819	-1
8c	4	-62.5	-36.5	0.236	0.461187	68.589	0.469602	71.437	1
7a	24	37.5	36.5	0.166	0.320259	29.479	0.330680	30.538	1
7b	8	-37.5	-13.5	0.166	0.320259	150.521	0.330680	149.462	-1
7c	28	37.5	-59.5	0.166	0.325344	91.059	0.325344	88.941	-1
6a	15	-12.5	-50.5	0.117	0.229395	50.572	0.225614	49.437	-1
6b	27	37.5	-36.5	0.117	0.230433	169.870	0.224640	170.127	1
6c	31	62.5	-13.5	0.117	0.228493	109.301	0.226482	110.693	1
5a	6	-37.5	36.5	0.083	0.158505	69.515	0.159487	70.488	1
5b	30	62.5	13.5	0.083	0.160427	10.091	0.157598	9.911	-1
5c	2	-62.5	13.5	0.083	0.158078	130.394	0.159925	129.601	-1
4a	25	37.5	13.5	0.059	0.111198	89.638	0.111198	90.362	1
4b	5	-37.5	59.5	0.059	0.110594	29.820	0.111811	30.182	1
4c	23	37.5	59.5	0.059	0.110594	150.180	0.111811	149.818	-1
3a	7	-37.5	13.5	0.042	0.077582	110.237	0.077817	109.762	-1
3b	29	62.5	36.5	0.042	0.077921	50.194	0.077480	49.807	-1
3c	1	-62.5	36.5	0.042	0.078039	169.956	0.077364	170.044	1
2a	12	-12.5	50.5	0.030	0.054408	129.864	0.054192	130.135	1
2b	19	12.5	27.5	0.030	0.054357	70.166	0.054243	69.834	-1
2c	17	12.5	73.5	0.030	0.054136	9.969	0.054465	10.031	1
1a	11	-12.5	73.5	0.022	0.037929	150.062	0.038071	149.938	-1
1b	13	-12.5	27.5	0.022	0.038000	90.124	0.038000	89.876	-1
1c	18	12.5	50.5	0.022	0.037929	29.938	0.038071	30.062	1

Table 1. Nominal values of the parameters charactering each sub–collimator. *From left to right*: sub–collimator label, sub–collimator number, coordinates of the window center, slit width, pitch of the front window, orientation angle of the front window, pitch of the rear window, orientation angle of the rear window and m factor. The values of the center coordinates and of the slit width are the same for the front and the rear window of the same sub–collimator. The parameters of windows 9 and 10 are not reported, as they refer to CFL and BKG, respectively.

Paolo Ma ... a Francesco
Battaglia[3], ... Garbarino[1,7],
Sabrina Gu ... Ryan[3], Shane
A. Malo ... Massone[1],
2

ground software

A&A 668, A145 (2022)
https://doi.org/10.1051/0004-6361/202243907

Astronomy & Astrophysics

Forward fitting STIX visibilities

Anna Volpara[1], Paolo Massa[2], Emma Perracchione[3], Andrea Francesco Battaglia[5,6], Sara Garbarino[1], Federico Benvenuto[1], Säm Krucker[5,7], Michele Piana[1,8], and Anna Maria Massone[1,4]

first science results

Solar Physics (2023) 298:1
https://doi.org/10.1007/s11207-022-02090-6

Check for updates

The Eruption of 22 April 2021 as Observed by Solar Orbiter: Continuous Magnetic Reconnection and Heating After the Impulsive Phase

L. Rodriguez[1] · A. Warmuth[2] · V. Andretta[3] · M. Mierla[1,4] · A.N. Zhukov[1,5] · D. Shukhobodskaia[1] · A. Niemela[6,1] · A. Maharana[6,1] · M.J. West[7] · E.K.J. Kilpua[8] · C. Möstl[9] · E. D'Huys[1] · A.M. Veronig[10] · F. Auchère[11] · A.F. Battaglia[12,13] · F. Benvenuto[14] · D. Berghmans[1] · E.C.M. Dickson[10] · M. Dominique[1] · S. Gissot[1] · L.A. Hayes[15] · A.C. Katsiyannis[1] · E. Kraaikamp[1] · F. Landini[16] · J. Magdalenić[1,6] · G. Mann[2] · P. Massa[17] · B. Nicula[1] · M. Piana[14] · O. Podladchikova[2] · C. Sasso[3] · F. Schuller[2] · K. Stegen[1] · R. Susino[16] · M. Uslenghi[18] · C. Verbeeck[1]

STIX: principle and physics

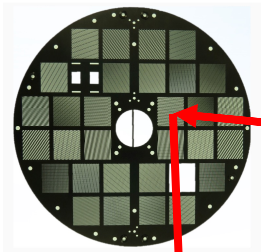

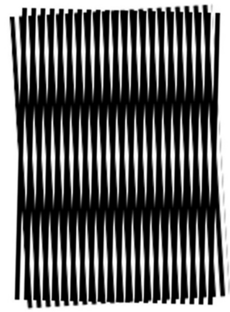

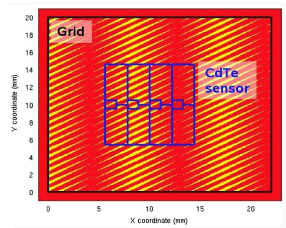

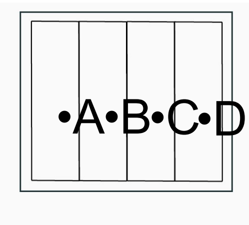

$$V(\xi) \simeq \frac{1}{4M_1}[(\boldsymbol{C}-\boldsymbol{A})+i(\boldsymbol{D}-\boldsymbol{B})]\exp\left(i\frac{\pi}{4}\right)$$

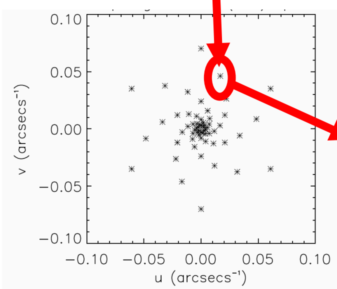

$$\xi = \mathrm{k}^f \frac{L_1+L_2}{S} - \mathrm{k}^r \frac{L_2}{S}$$

$$V(\xi) = \int_{\mathbb{R}^2} \phi(\mathbf{x}) \exp(2\pi i \xi \cdot \mathbf{x})\, d\mathbf{x}.$$

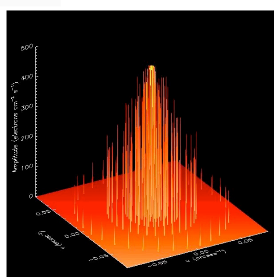

AI

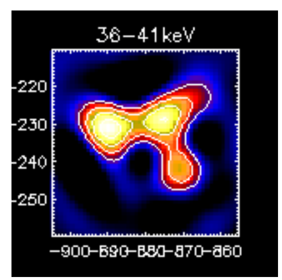

STIX observes count visibilities

count visibilities are directly connected to photons

physics is in the electrons

from photon to electron visibilities

- photon visibilities:

$$V(u,v;\varepsilon) = \iint I(x,y;\varepsilon)\, e^{2\pi i(ux+vy)}\, dxdy$$

- bremsstrahlung equation:

$$I(x,y;\varepsilon) = \frac{a^2}{4\pi R^2} \int_{\varepsilon}^{\infty} N(x,y)\overline{F}(x,y;E)Q(\varepsilon,E)\,dE$$

- electron visibilities:

$$W(u,v;E) := \frac{a^2}{4\pi R^2} \iint N(x,y)\overline{F}(x,y;E)\, e^{2\pi i(ux+vy)}\, dxdy$$

- bremsstrahlung equation for visibilities

$$V(u,v;\varepsilon) = \int_{\varepsilon}^{\infty} W(u,v;E)Q(\varepsilon,E)\,dE$$

from photon to electron visibilities

$$V(u,v;\varepsilon) = \int_{\varepsilon}^{\infty} W(u,v;E)\,Q(\varepsilon,E)\,dE$$

the relation between the **measured photon visibilities** and the **electron visibilities** is described by a Volterra integral equation of the first kind

visibility inversion problem: determine the electron visibilities, *W(u,v;E)*, from the observed count visibilities *V(u,v;ε)*

visibility information in photon space may be converted,
via a (regularized) spectral inversion technique,
to visibility information in the *electron* domain.

electron maps

algorithm for electron image reconstruction:

1. for each (u,v) pair solve

$$V(u,v;\varepsilon) = \int_{\varepsilon}^{\infty} W(u,v;E) Q(\varepsilon,E)\, dE$$

by means of tikhonov regularization (which regularizes along the energy direction)

2. for each E solve

$$W(u,v;E) = \frac{a^2}{4\pi R^2} \iint \overline{F}(x,y;E) e^{2\pi i(ux+vy)}\, dx\, dy$$

by means of a fourier-based imaging algorithm (which reduces artifacts by imposing appropriate constraints)

(piana et al, electron flux spectral imaging of solar flares through regularized analysis of hard X-ray source visibilities, ApJ, 665, 846, 2007)

visibility inversion algorithm: implementation

$$
\begin{array}{c|ccccc|}
 & \varepsilon_1 & \varepsilon_2 & \cdots & & \varepsilon_N \\
\hline
(u_1, v_1) & V_{1,1} & V_{1,2} & \cdots & & V_{1,N} \\
(u_2, v_2) & V_{2,2} & \cdots & \cdots & \cdots & \\
\vdots & \vdots & \ddots & & & \vdots \\
(u_V, v_V) & V_{V,V} & \cdots & \cdots & & V_{V,N} \\
\hline
\end{array}
$$

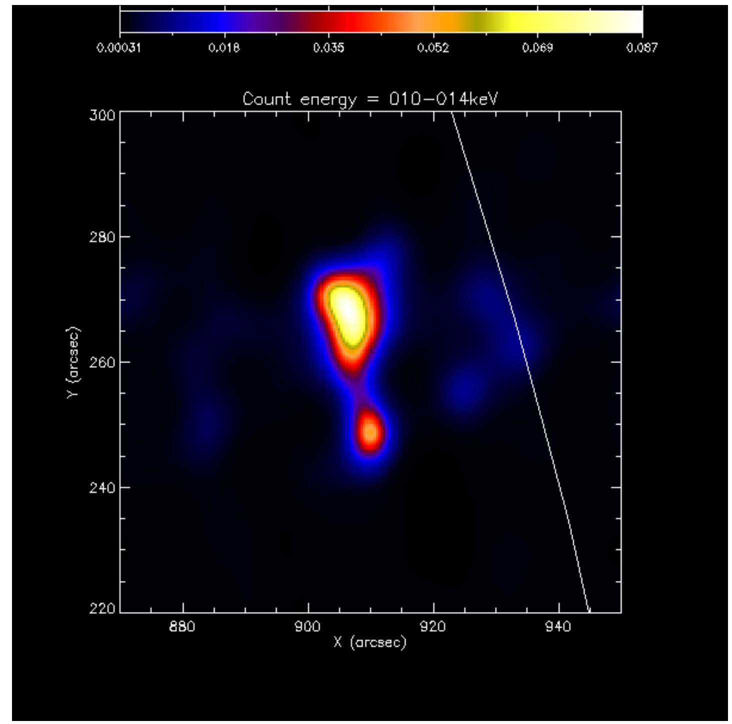

(prato et al regularized visibility-based approach to astronomical imaging spectroscopy SIAM journal im sci, 2 910, 2009)

visibility inversion algorithm: implementation

$$
\begin{array}{c|cccc|}
 & \varepsilon_1 & \varepsilon_2 & \cdots & \varepsilon_N \\
\hline
(u_1, v_1) & V_{1,1} & V_{1,2} & \cdots & V_{1,N} \\
(u_2, v_2) & V_{2,2} & & \cdots & \\
\vdots & \vdots & & \ddots & \vdots \\
(u_V, v_V) & V_{V,V} & & \cdots & V_{V,N} \\
\hline
\end{array}
$$

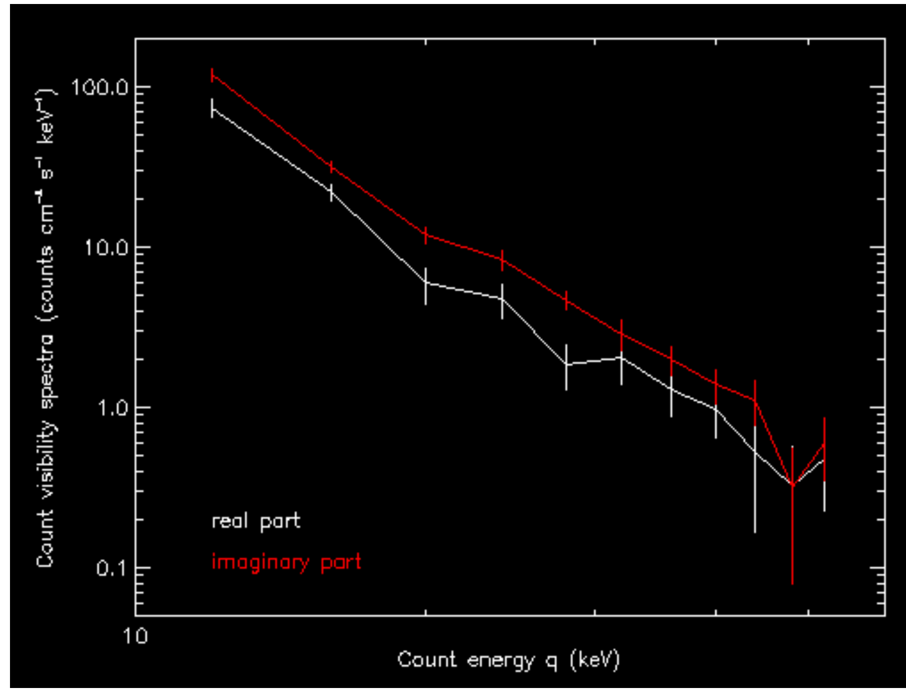

$$V(u_1, v_1; \varepsilon)$$

visibility inversion algorithm: implementation

$$
\begin{array}{c|cccc|}
 & \varepsilon_1 & \varepsilon_2 & \cdots & \varepsilon_N \\
\hline
(u_1, v_1) & V_{1,1} & V_{1,2} & \cdots & V_{1,N} \\
(u_2, v_2) & V_{2,2} & \cdots & \cdots & \cdots \\
\vdots & \vdots & & \ddots & \vdots \\
(u_V, v_V) & V_{V,V} & \cdots & \cdots & V_{V,N} \\
\hline
\end{array}
$$

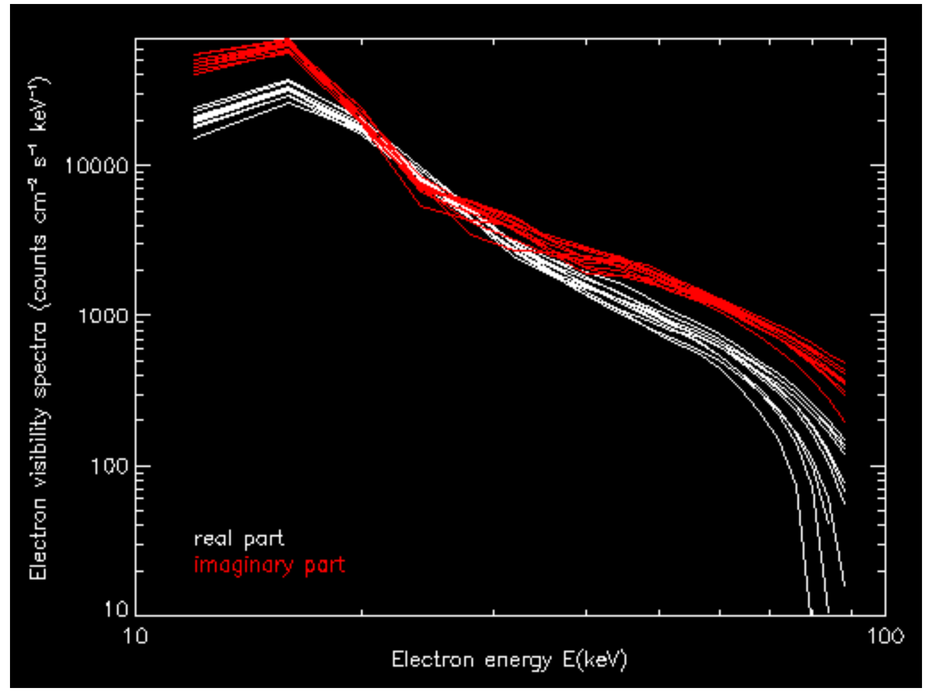

$$W(u_1, v_1; E)$$

visibility inversion algorithm: implementation

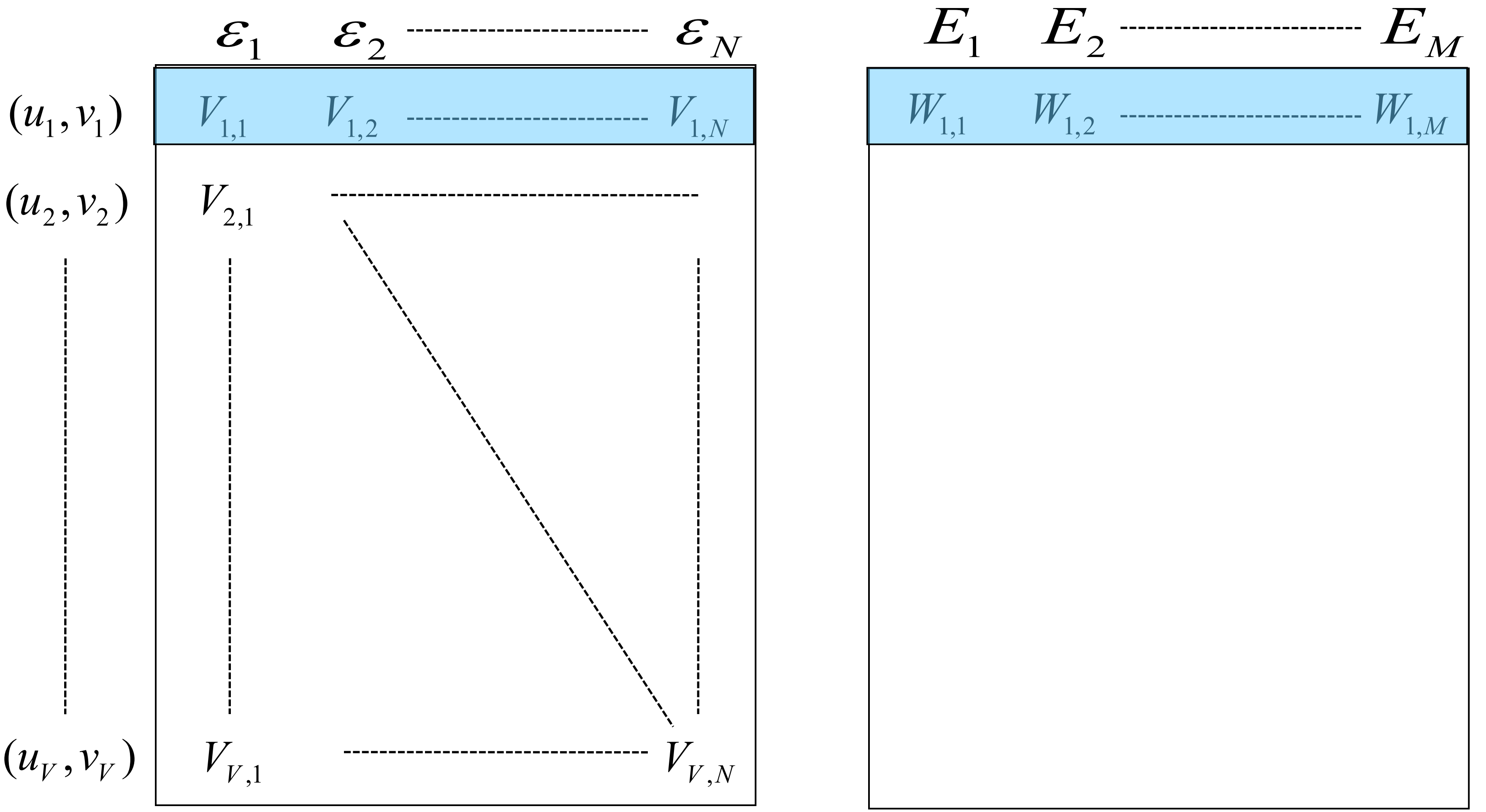

from electron visibilities to electron maps

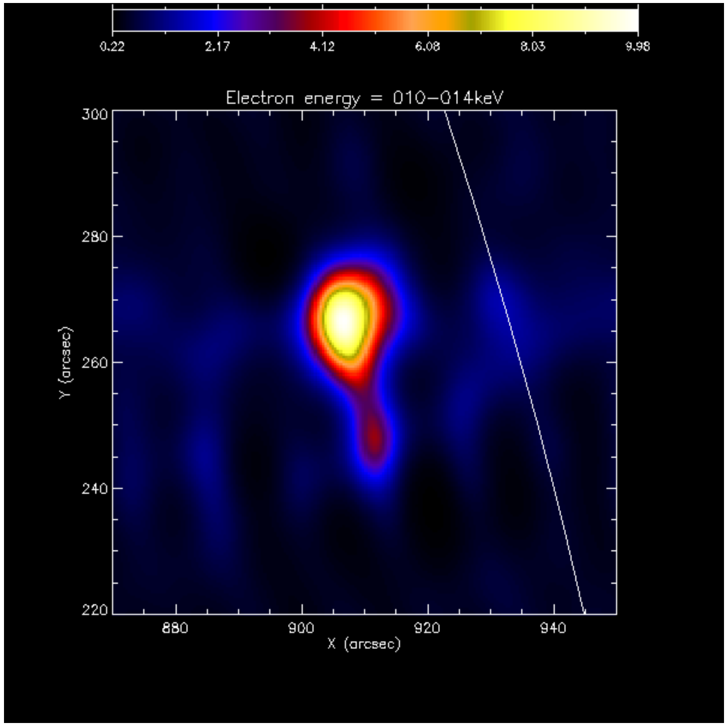

$$\begin{array}{cccc} E_1 & E_2 & \cdots & E_M \\ W_{1,1} & W_{1,2} & \cdots & W_{1,M} \\ W_{2,1} & \cdots & \cdots & \cdots \\ \vdots & \ddots & & \vdots \\ W_{V,1} & \cdots & \cdots & W_{V,M} \end{array}$$

STIX photon vs electron maps: may 7 2021

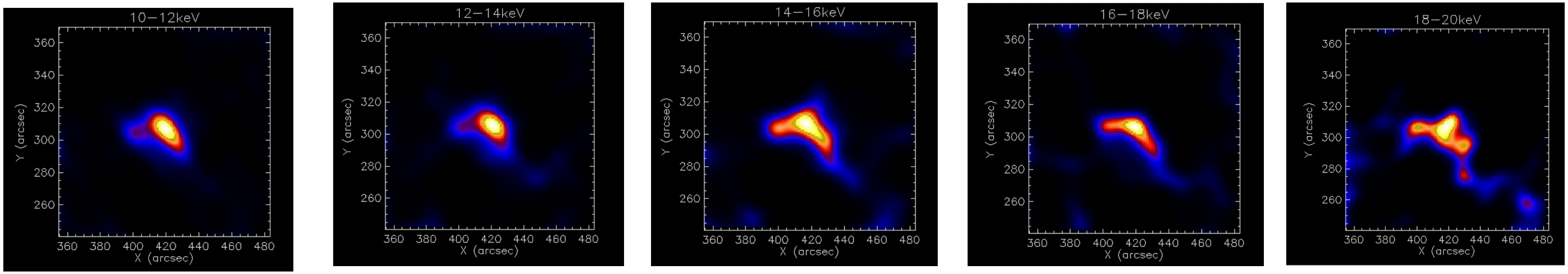

10-12 keV　12-14 keV　14-16 keV　16-18 keV　18-20 keV

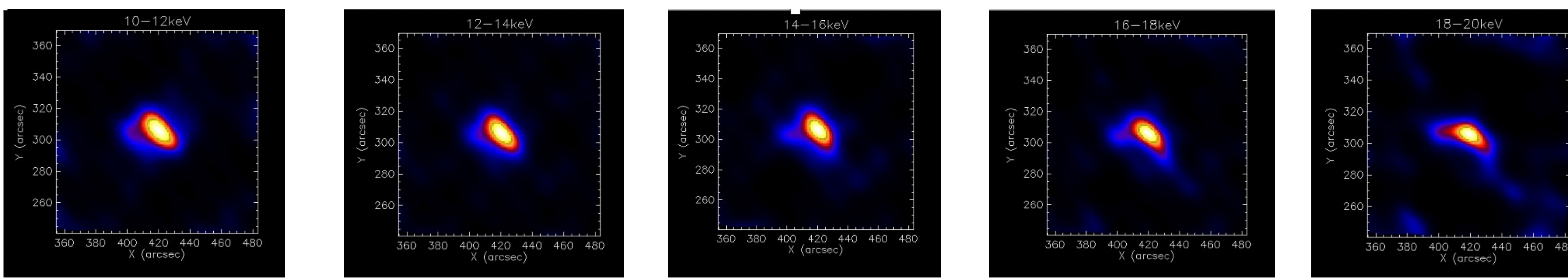

imaging method: massa et al, MEM GE: a new maximum entropy method for image reconstruction from solar X-ray visibilities, ApJ, 894, 46, 2019

photon vs electron maps: may 7 2021

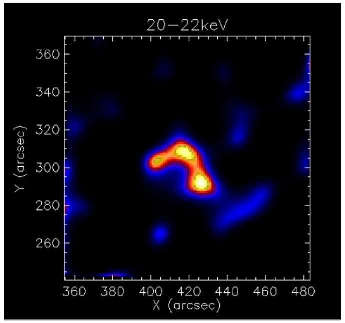

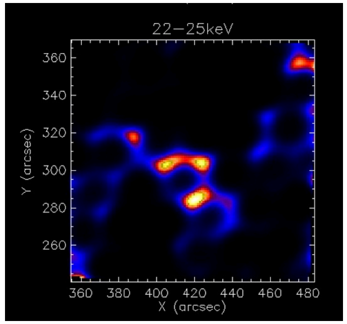

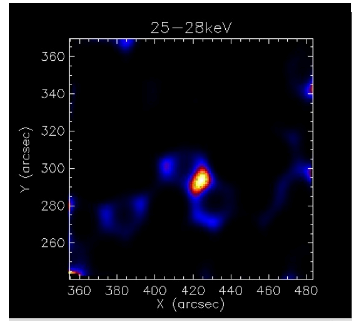

20-22 keV 22-25 keV 25-28 keV 28-32 keV 32-36 keV

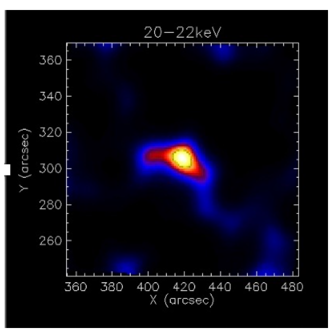

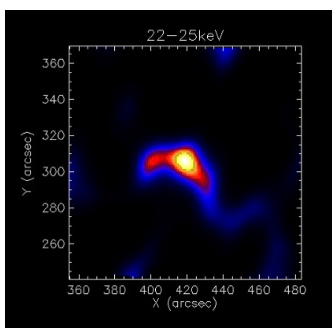

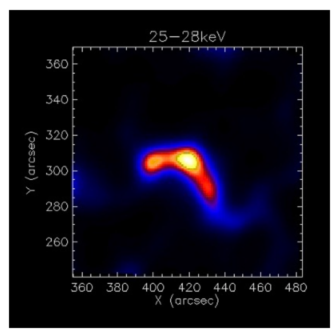

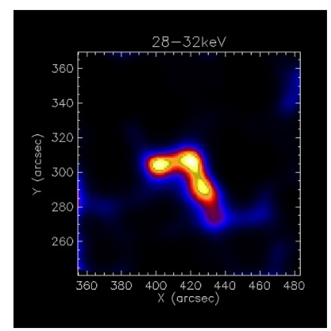

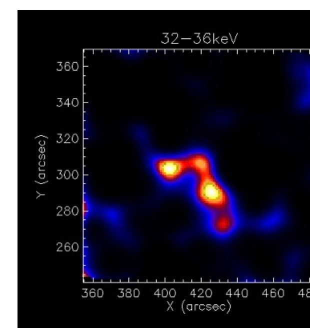

photon vs electron maps: may 7 2021

36-40 keV

40-45 keV

45-50 keV

50-56 keV

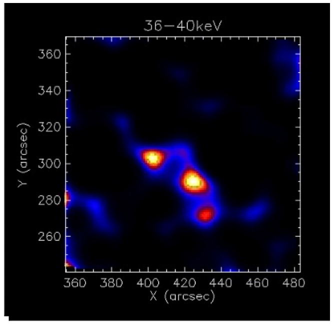

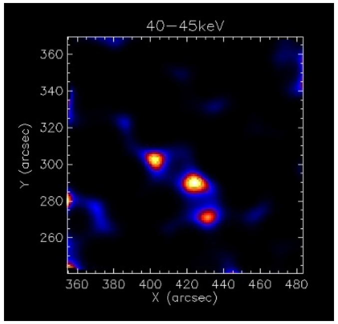

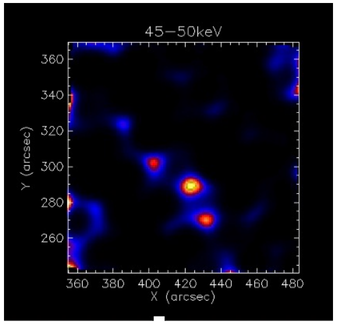

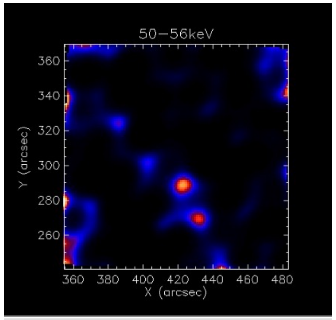

APPLICABILITY CONDITIONS – FROM RHESSI TO STIX

this software realizes an imaging spectroscopy procedure, i.e. it provides electron visibility cubes from photon visibility cubes. specifically:

• you need count visibilities at many count energies

• you do not necessarily need uniform sampling of the count energies (differently than what required in the RHESSI GUI)

• the output electron energies have the same sampling of the count energies

• you will have more output electron energies than input count energies

• the software also produces regularized photon maps

• differently than for RHESSI, you have as many electron visibility spectra as count visibility spectra

in progress: DEM maps

$$\phi(\epsilon) = \int_\epsilon^\infty F(E) Q(\epsilon, E) dE \qquad F(E) = \int_V n(r) \mathcal{F}(E, r) dr$$

$$\mathcal{F}(E, r) = A \frac{n(r) E}{[kT(r)]^{3/2}} e^{-\frac{E}{kT(r)}}$$

$$F(E) = AE \int_V \frac{n^2(r)}{[kT(r)]^{3/2}} e^{-\frac{E}{kT(r)}} dr$$

$$dr = dS_T dl = \frac{1}{|\nabla T|} dS_T dT$$

$$F(E) = AE \int_0^\infty \xi(T) \frac{e^{-\frac{E}{kT}}}{[kT]^{3/2}} dT \qquad \xi(T) = \int_{S_T} \frac{n^2(r(T))}{|\nabla T|} dS_T$$

$$Q(\epsilon, E) = \frac{1}{\epsilon E}$$

$$\phi(\epsilon) = \frac{A}{\epsilon} \int_0^\infty \xi(T) \frac{e^{-\frac{E}{kT}}}{(kT)^{1/2}} dT \qquad \phi(x, y; \epsilon) = \frac{A}{\epsilon} \int_0^\infty \xi(x, y; T) \frac{e^{-\frac{E}{kT}}}{(kT)^{1/2}} dT$$

$$V(u, v; \epsilon) = \int \int \phi(x, y; \epsilon) e^{i(xu+yv)} dx dy \qquad W(u, v; T) = \int \int \xi(x, y; T) e^{i(xu+yv)} dx dy$$

$$V(u, v; \epsilon) = \frac{A}{\epsilon} \int_0^\infty W(u, v; T) \frac{e^{-\frac{E}{kT}}}{(kT)^{1/2}} dT$$

more in progress: energy budget

released energy	flare	hard X-rays	STIX
thermal energy	chromosphere/corona	EUV	EUI
kinetic energy	corona	CME	METIS

ingredients:

- event with both flare and CME
- limb flare observation
- (possibly) some de-saturation at EUV
- algorithms for parameter estimation

emslie et al,
global energetics of thirty-eight large solar eruptive events,
ApJ, 759, 71, 2012

even more in progress: coronal holes

correlations between coronal holes and solar wind variations:

- hard X-ray emission from the corona: STIX
- coronal holes: EUI
- solar wind: SWA

- bale et al, highly structured slow solar wind emerging from an equatorial coronal hole, nature, 576, 237, 2019
- krucker et al, hard X-ray emission from the solar corona, astron. astrophys. rev., 16, 155, 2008